Dynamics, Control and Secure Transmission Electronic Circuit Implementation of a New 3D Chaotic System in Comparison With 50 Reported Systems

KHALED BENKOUIDER [ID][1], **TOUFIK BOUDEN**[1], **ACENG SAMBAS**[2], **MOHAMAD AFENDEE MOHAMED** [ID][3], (Associate Member, IEEE), **IBRAHIM MOHAMMED SULAIMAN** [ID][4], **MUSTAFA MAMAT**[3], **AND MOHD ASRUL HERY IBRAHIM**[5]

[1]Automatic Department, University of Jijel, Ouled Aissa, Jijel 18000, Algeria
[2]Department of Mechanical Engineering, Universitas Muhammadiyah Tasikmalaya, Tasikmalaya, West Java 46196, Indonesia
[3]Faculty of Informatics and Computing, Universiti Sultan Zainal Abidin, Kuala Terengganu 21300, Malaysia
[4]Department of Mathematics and Statistics, School of Quantitative Sciences, College of Art and Sciences, Universiti Utara Malaysia, Kedah 06010, Malaysia
[5]Faculty of Entrepreneurship and Business, Universiti Malaysia Kelantan, Kota Bharu, Kelantan 16100, Malaysia

Corresponding author: Mohamad Afendee Mohamed (mafendee@unisza.edu.my)

ABSTRACT The very high demand for chaotic systems in the fields of sciences, particularly in secure communication, leads numerous researchers to build novel systems. This work announces a new easy to implement 3D chaotic system with five quadratic nonlinearities and three positive parameters, the proposed system is complex with larger bandwidth compared to at least 50 other systems that have been described. It contains eight terms and it can generate chaotic, periodic and quasi-periodic behaviors. The main dynamical properties of the proposed system are studied using Kaplan-Yorke dimension (KYD), Lyapunov exponents, bifurcation diagrams, multistability, equilibrium points stability and dissipativity. Then, the eight terms system feasibility is verified using Multisim software by designing its electronic circuit. In addition, active controllers are designed for leading the proposed system to achieve stability, tracking a desired dynamic and synchronizing with an identical model. Finally, using drive response synchronization, a novel secure communication electrical circuit design is built based on the suggested approach. The findings from numerical experiment demonstrated the new system's success in completing the encryption/decryption process, as well as its secured transmission technique.

INDEX TERMS Bandwidth, chaotic communication, chaotic systems, circuit Simulation, command and control systems.

I. INTRODUCTION

After Lorenz first developed Lorenz chaotic system in 1963 [1], which proved that a three-dimensional system can generate a chaotic behavior with one positive Lyapunov exponent; many other chaotic systems was introduced in literature based on the Lorenz model or by constructing new models [2]–[8].

Chaotic systems are applicable in several fields, including secure communication schemes [9]–[11], physics [12], robotics [13], economy [14], lasers [15] and ecology [16].

Which make the construction of new chaotic systems an obligatory in line with the current demand for complex systems of this kind.

In addition, since the famous work of Pecora and Caroll [17], which proved the possibilities of synchronizing two identical chaotic systems having different initial guess, many of synchronization methods are employed for synchronizing chaotic systems, which include backstopping control [18], sliding mode control [19], adaptive control [20], active control [21], and so on.

In the current digital age, there has been a lot of interest on secure communication links due to the dramatic rise of online shopping, banking and trading transaction and this

The associate editor coordinating the review of this manuscript and approving it for publication was Wenjie Feng.

trend is set to increase exponentially in future [22]. In effect, it does not take much effort to realize that there will be a significant increase of users of digital communication and technology in the next decade and further. Consequently, for chaos-based communication, there is a need to develop new chaotic systems with large bandwidth in order to cover the secure communication between the huge numbers expected of users.

Also, the existence of multistability phenomenon in certain chaotic systems is very interesting, it is means that the system not only exhibits chaotic behaviour with extreme sensitivity to the initial values; but also it can generate coexistence of different chaotic attractors depending only on its initial conditions. Multistability making a chaotic system more complex and more useful to use in many application that require complexity, especially in secure communication.

This study suggested the first new and easy to implement 3D chaotic system with five quadratic nonlinearities which is more complex and has larger bandwidth than at least 50 other systems that have been described, major properties of the announced system are investigated via theoretical and analytical methods. Also, Multisim software is used in designing and realizing an electronic circuit with the aim of validating the developed 3D model. In addition, active controllers are designed for leading the proposed system to achieve stability, tracking a desired dynamic and synchronizing. Finally, using drive response synchronization, a novel secure communication electrical circuit design is built based on the new announced system.

The rest part of the paper is designed as follows: In section 2, dynamical properties of the proposed system have been investigated using Kaplan-Yorke dimension, Lyapunov exponents, bifurcation diagrams, dissipativity, multistability and equilibrium points stability, also a comparison of the suggested system with 50 previously reported systems is introduced in section 3. The circuit schematic of the new model is realized using Multisim software in section 4. In section 5, active controllers are designed and applied to control the new system. Also, a new secure communication electronic circuit schematic is implemented based on the suggested three-dimensional chaotic system. Lastly, conclusions are dressed in section 6.

II. DYNAMICAL PROPERTIES OF THE NEW SYSTEM
A. NEW CHAOTIC SYSTEM
The new 3D chaotic system contains eight terms with five quadratic nonlinearities and three positive constant parameters defined by the algebraic equations that follows:

$$\begin{cases} \dot{x}_1 = -ax_1x_3 + bx_2(1 - x_3) \\ \dot{x}_2 = cx_1x_3 - x_1^2 \\ \dot{x}_3 = -x_1 - x_3 + x_2^2 \end{cases} \quad (1)$$

where the state variables denoted by x_1, x_2 and x_3 while a, b and c are the positive constant coefficients. By choosing (1, 1, 1) as the initial conditions and $a = 1.1$, $b = 13$ and $c = 11$ as the parameters values; the proposed
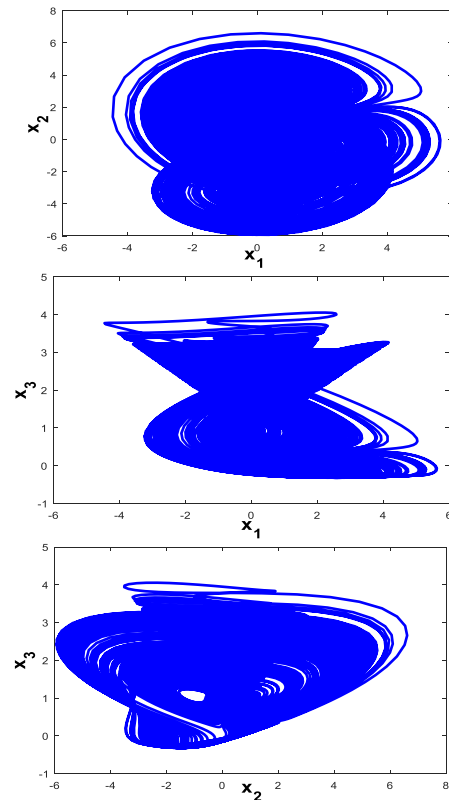

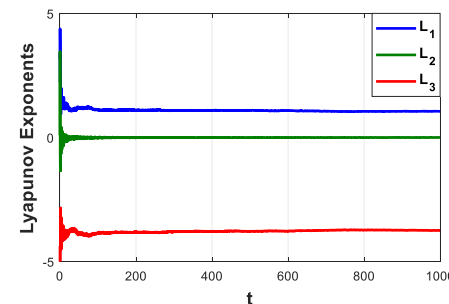**FIGURE 1.** Chaotic attractors of the new system (1).

FIGURE 2. Lyapunov exponents of the new system (1).

system (1) exhibit a complex chaotic behavior as depicted in Figure 1.

For the previous parameters values, the Lyapunov exponents of system (1) are obtained using Wolf's algorithm, results are shown in Figure 2 as:

$$L_1 = 1.051, \quad L_2 = 0.000, \quad L_3 = -3.745 \quad (2)$$

As depicted in Figure 2 there are one negative exponent, one zero exponent, and one positive Lyapunov exponents. So, the suggested system is chaotic, and the corresponding KYD is computed as follow:

$$D_{KY} = 2 + \frac{L_1 + L_2}{|L_3|} = 2.281 \quad (3)$$

TABLE 1. Equilibrium points stability.

E_i	$J(E_i)$ eigenvalues	Stability
E_1	$\lambda_1 = 0, \ \lambda_2 = 0, \ \lambda_3 = -1$	Unstable
E_2	$\lambda_1 = -9.286, \ \lambda_2 = 2.143 + 5.119i, \ \lambda_3 = 2.143 - 5.119i$	Unstable
E_3	$\lambda_1 = -7.657, \ \lambda_2 = 1.329 + 5.965i, \ \lambda_3 = 1.329 - 5.965i$	Unstable

The KYD is fractional, implying that the new eight terms system (1) demonstrate a complicated chaotic behavior.

B. EQUILIBRIUM POINTS STABILITY

The following equations are used to determine the points of equilibrium of the suggested system (1):

$$\begin{cases} -ax_1x_3 + bx_2(1 - x_3) = 0 \\ cx_1x_3 - x_1^2 = 0 \\ -x_1 - x_3 + x_2^2 = 0 \end{cases} \quad (4)$$

By considering the previous values of parameters, three equilibrium points is obtained as the following:

$$E_1 = \begin{bmatrix} 0 \\ 0 \\ 0 \end{bmatrix}, \quad E_2 = \begin{bmatrix} 0 \\ 1 \\ 1 \end{bmatrix}, \quad E_3 = \begin{bmatrix} 0 \\ -1 \\ 1 \end{bmatrix} \quad (5)$$

The Jacobian system (1) is described as:

$$J(E_i) = \begin{bmatrix} -ax_3 & b - bx_3 & -ax_1 - bx_2 \\ cx_3 - 2x_1 & 0 & cx_1 \\ -1 & 2x_2 & -1 \end{bmatrix} \quad (6)$$

We can investigate the stability nature of the new chaotic system (1) by linearizing it at each point of equilibrium using the following characteristic equation:

$$|J(E_i) - \lambda I| = 0 \ \text{ and } \ i = 1, \ 2, \ 3 \quad (7)$$

Table 1 demonstrate the chaos in the dissipative system due to the instability of all the equilibrium points.

C. DISSIPATIVITY

The sum of Lyapunov exponents (2) is negative, so it is clear that the proposed eight terms system defined by (1) is dissipative. Therefore, orbits of the whole of system (1) are ultimately constricted to a particular subset of zero volume, and the asymptotic motion relaxes on a chaotic attractor.

D. BIFURCATION ANALYSIS

The bifurcation parameter a versus system (1) dynamical behaviors is analyzed using Lyapunov exponents spectrum and bifurcation diagram presented in Figures 3 and 4, respectively, as parameter a varies.

It can be seen from Figure 3 and 4 that the proposed model has a rich dynamical behavior, as it can show chaotic behavior, periodic and quasi-periodic behaviors when parameter a increase as summarized in Table 2.
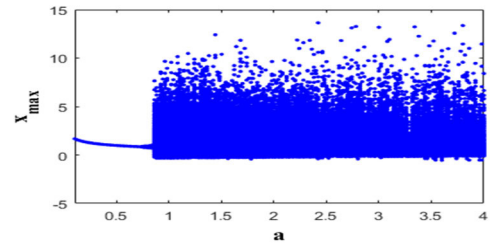

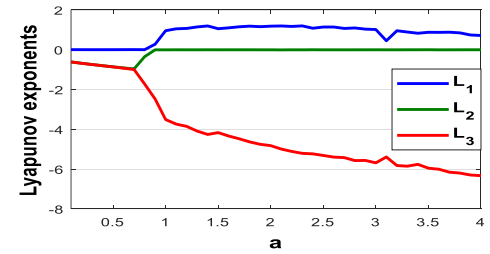**FIGURE 3.** Bifurcation diagram of system (1) first state versus parameter a.

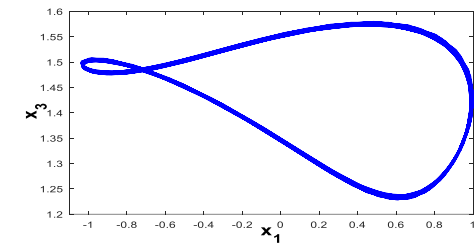**FIGURE 4.** Lyapunov exponents spectrum of system (1) versus parameter a.

FIGURE 5. Phase portraits of the periodic orbit for $a = 0.5$.
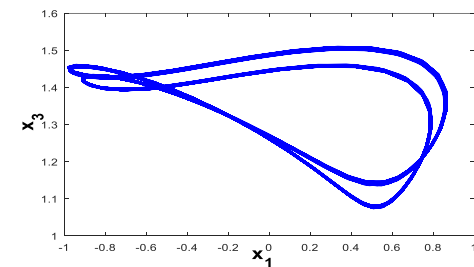

**FIGURE 6.** Phase portraits of the quasi-periodic orbit for $a = 0.8$.

E. FREQUENCY SPECTRUM AND BANDWIDTH

The bandwidth of a chaotic system should be large in order to completely cover the masked signal in chaos-based secure transmission applications. This is not the case in many of reported chaotic systems, which the frequency spectrum of its signals is not broad enough. Therefore, it is of great significance to construct new chaotic systems with larger bandwidth than existing ones.

Figure 8 shows the normalised average frequency spectrum of the signal generated by the second state variable x_2 of system (1), The novel chaotic system has a bandwidth (BWT)

TABLE 2. Dynamical behaviors of system (1).

a	*Lyapunov exponents*	Dynamics	Figure
$0.5 \in [0, 0.7]$	$L_1 = 0.00$, $L_2 = -0.86$, $L_3 = -0.861$	Periodic	5
0.8	$L_1 = 0.00$, $L_2 = 0.00$, $L_3 = -1.72$	Quasi-periodic	6
$2 \in [0.9, 4]$	$L_1 = 1.196$, $L_2 = 0.00$, $L_3 = -4.81$	Chaotic	7
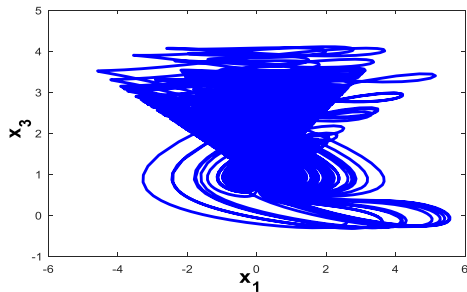
FIGURE 7. Phase portraits of the chaotic attractor for $a = 2$.
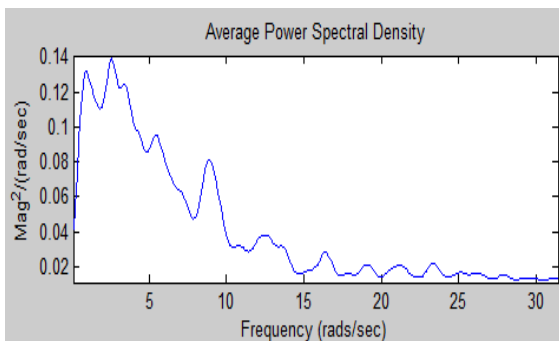
FIGURE 8. Average power spectrum of the first state signal x_2.

of about 15, that is greater when compared it to more than 50 chaotic systems documented in the study, indicated in Table 3.

F. MULTISTABILITY AND COEXISTING ATTRACTORS

Let X_0, Y_0 be two different initial values for the new 3-D system (1), where:

$X_0 = (-1, -1, 2)$ (Blue color)

$Y_0 = (-2, 0, 3)$ (Red color)

Fix $b = 13$, $c = 11$ and vary a, it can be proved from the numerical simulations that the new 3-D system (1) is multistable. When $a = 0.9$, we can see from Figure 9 that system (1) has coexistence of two different chaotic attractors starting from X_0 and Y_0 for the same values of parameters. Coexistence of one chaotic attractor and one periodic attractor starting from Y_0 and X_0 respectively are determined when $a = 9.6$ as depicted in Figure 10. When $a = 6.6$, we can
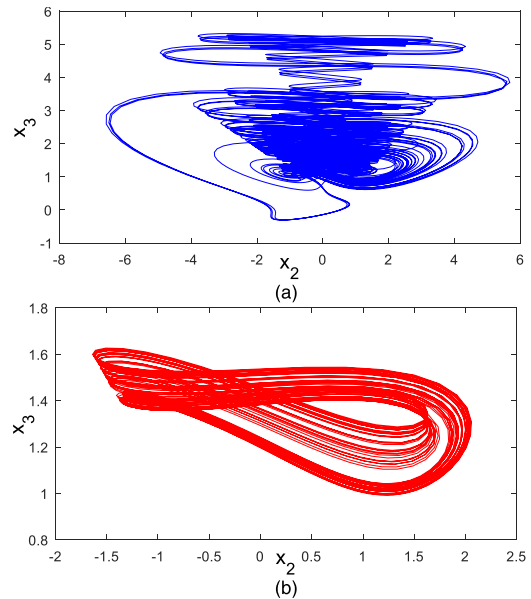
FIGURE 9. Coexistence of two different chaotic attractors projected on the x_2-x_3 plane when $a = 0.9$ and starting from: (a) X_0 (blue) and (b) Y_0 (red).
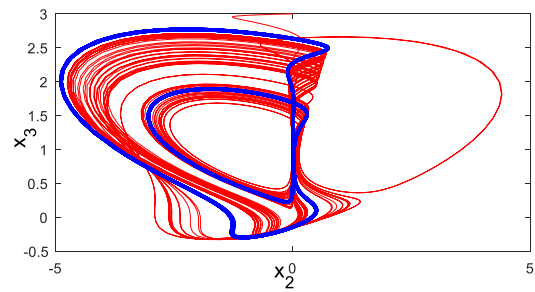
FIGURE 10. Coexistence of one chaotic attractor and one periodic attractor projected on the x_2-x_3 plane when $a = 9.6$ and starting from: X_0 (blue) and Y_0 (red).
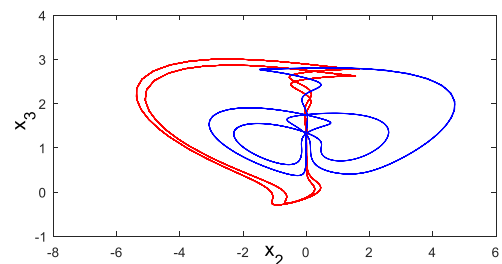
FIGURE 11. Coexistence of two different periodic attractors projected on the x_2-x_3 plane when $a = 6.6$ and starting from: X_0 (blue) and Y_0 (red).

see from Figure 11 that system (1) has coexistence of two different periodic attractors starting from X_0 and Y_0 for the same values of parameters.

The obtained results enable us to observe the phenomenon of multistability, this strange phenomenon proves the high complexity of the new system (1), which make it very suitable to use in engineering applications that require complexity; especially, chaos communication.

TABLE 3. Different reported chaotic systems with Kaplan-York dimension and bandwidth.

No.	System	Dynamics	KYD	BWT
1	Lorenz [25]	$\begin{cases} \dot{x}_1 = 10(x_2 - x_1) \\ \dot{x}_2 = 28x_1 - x_2 - x_1 x_3 \\ \dot{x}_3 = x_1 x_2 - 2.667 x_3 \end{cases}$	2.062	4
2	Chen [26]	$\begin{cases} \dot{x}_1 = 35(x_2 - x_1) \\ \dot{x}_2 = -x_1 x_3 - 7x_1 + 28x_2 \\ \dot{x}_3 = -3x_3 + x_1 x_2 \end{cases}$	2.175	6
3	Rossler |27]	$\begin{cases} \dot{x}_1 = -x_2 - x_3 \\ \dot{x}_2 = x_1 + 0.2x_2 \\ \dot{x}_3 = 0.2 + x_3(x_1 - 5.7) \end{cases}$	2.013	1
4	Chen et al. [28]	$\begin{cases} \dot{x}_1 = 4.6x_1 + x_2 - x_2 x_3 \\ \dot{x}_2 = x_1 x_3 - x_3 - 12x_2 \\ \dot{x}_3 = -x_1 - 5x_3 + x_1 x_2 \end{cases}$	2.010	8.5
5	Li [29]	$\begin{cases} \dot{x}_1 = 40(x_2 - x_1 + 0.16x_1 x_3) \\ \dot{x}_2 = 55x_1 - 20x_2 - x_1 x_3 \\ \dot{x}_3 = -0.65x_1^2 + x_1 x_2 + 1.83x_3 \end{cases}$	2.112	5
6	Zhou et al. [30]	$\begin{cases} \dot{x}_1 = 10(x_2 - x_1) \\ \dot{x}_2 = 16x_1 - x_1 x_3 \\ \dot{x}_3 = x_1 x_2 - x_3 \end{cases}$	2.097	3
7	Lu [31]	$\begin{cases} \dot{x}_1 = 36(x_2 - x_1) \\ \dot{x}_2 = 20x_2 - x_1 x_3 \\ \dot{x}_3 = x_1 x_2 - 3x_3 \end{cases}$	2.066	7
8	Lorenz [32]	$\begin{cases} \dot{x}_1 = 16(x_2 - x_1) \\ \dot{x}_2 = 45.92x_1 - x_2 - x_1 x_3 \\ \dot{x}_3 = x_1 x_2 - 2.667x_3 \end{cases}$	2.066	6
9	Lorenz [33]	$\begin{cases} \dot{x}_1 = 10(x_2 - x_1) \\ \dot{x}_2 = 142x_1 - x_2 - x_1 x_3 \\ \dot{x}_3 = -2.667x_3 + x_1 x_2 \end{cases}$	2.089	7
10	Cai et al. [34]	$\begin{cases} \dot{x}_1 = 20(x_2 - x_1) \\ \dot{x}_2 = 14x_1 + 10.6x_2 - x_1 x_3 \\ \dot{x}_3 = x_1^2 - 2.8x_3 \end{cases}$	2.164	6
11	Tigan et al. [35]	$\begin{cases} \dot{x}_1 = 2.1(x_2 - x_1) \\ \dot{x}_2 = 30x_1 - x_2 - x_1 x_3 \\ \dot{x}_3 = x_1 x_2 - 0.6x_3 \end{cases}$	2.121	1
12	Modified Lu [36]	$\begin{cases} \dot{x}_1 = 35(x_2 - x_1 + x_2 x_3) \\ \dot{x}_2 = 14x_2 - x_1 x_3 \\ \dot{x}_3 = x_1 x_2 - 5x_3 \end{cases}$	2.034	7

AQ:6

TABLE 3. *(Continued.)* Different reported chaotic systems with Kaplan-York dimension and bandwidth.

13	Liu et al. [37]	$\begin{cases}\dot{x}_1 = 10(x_2 - x_1)\\ \dot{x}_2 = 40x_1 - x_1 x_3\\ \dot{x}_3 = 4x_2^2 - 2.5x_3\end{cases}$	2.116	1
14	Li et al. [38]	$\begin{cases}\dot{x}_1 = 5(x_2 - x_1)\\ \dot{x}_2 = 55x_1 - 5x_1 x_3\\ \dot{x}_3 = x_1 x_2 - 2x_3\end{cases}$	2.101	8
15	Munmuangsaen et al. [39]	$\begin{cases}\dot{x}_1 = 5(x_2 - x_1)\\ \dot{x}_2 = -x_1 x_3\\ \dot{x}_3 = x_1 x_2 - 90\end{cases}$	2.230	7
16	Liu et al. [40]	$\begin{cases}\dot{x}_1 = -x_2^2 - x_1\\ \dot{x}_2 = 2.5x_2 - 4x_1 x_3\\ \dot{x}_3 = 4x_1 x_2 - 5x_3\end{cases}$	2.119	2
17	Zhu et al. [41]	$\begin{cases}\dot{x}_1 = -x_1 - 1.5x_2 + x_2 x_3\\ \dot{x}_2 = 2.5x_2 - x_1 x_3\\ \dot{x}_3 = x_1 x_2 - 4.9x_3\end{cases}$	2.166	4
18	Liu et al. [42]	$\begin{cases}\dot{x}_1 = 10(x_2 - x_1)\\ \dot{x}_2 = 16x_1 - x_1 x_3\\ \dot{x}_3 = x_1 x_2 - 2.66x_3\end{cases}$	2.027	4
19	Pan [43]	$\begin{cases}\dot{x}_1 = 60(x_2 - x_1) + 0.4x_2 x_3\\ \dot{x}_2 = -35x_1 + 25x_2 - x_1 x_3\\ \dot{x}_3 = x_1 x_2 - 0.83x_3 - 0.65x_1^2\end{cases}$	2.063	5
20	Pehlivan [44]	$\begin{cases}\dot{x}_1 = (x_2 - x_1)\\ \dot{x}_2 = 0.5x_2 - x_1 x_3\\ \dot{x}_3 = x_1 x_2 - 0.5\end{cases}$	2.276	1
21	Wei et al. [45]	$\begin{cases}\dot{x}_1 = -x_2\\ \dot{x}_2 = x_1 + x_1\\ \dot{x}_3 = x_1 x_2 + 2x_2^2 - 0.35\end{cases}$	2.053	1
22	Li et al. [46]	$\begin{cases}\dot{x}_1 = 10(x_2 - x_1)\\ \dot{x}_2 = 6x_2 - x_1 x_3\\ \dot{x}_3 = x_2^2 - 3x_3\end{cases}$	2.057	2
23	Li et al. [47]	$\begin{cases}\dot{x}_1 = -16x_1 + 0.5x_2 x_3\\ \dot{x}_2 = 10x_2 - 6x_1 x_3\\ \dot{x}_3 = -5x_3 + 18x_2\end{cases}$	2.105	1
24	Kim et al. [48]	$\begin{cases}\dot{x}_1 = 30(x_2 - x_1)\\ \dot{x}_2 = 15x_2 + x_1 x_3\\ \dot{x}_3 = -x_1^2 - 11x_3\end{cases}$	2.033	3
25	Abooee [49]	$\begin{cases}\dot{x}_1 = 10(x_2 - x_1) + x_2 x_3^2\\ \dot{x}_2 = 5x_1 + x_1 x_3^2\\ \dot{x}_3 = -6x_1^2 - 5x_3\end{cases}$	2.037	6

TABLE 3. *(Continued.)* Different reported chaotic systems with Kaplan-York dimension and bandwidth.

26	Qiao et al. [50]	$\begin{cases} \dot{x}_1 = 10(x_2 - x_1) \\ \dot{x}_2 = -7x_2 - x_1 x_3 \\ \dot{x}_3 = -0.2x_1^2 + x_1 x_2 - 50 \end{cases}$	2.038	4
27	Deng et al. [51]	$\begin{cases} \dot{x}_1 = x_2 \\ \dot{x}_2 = x_3 - 0.5x_2 \\ \dot{x}_3 = -6x_1 - 2.85x_2 \end{cases}$	2.117	1
28	Gholizadeh [52]	$\begin{cases} \dot{x}_1 = 0.5x_2 x_3 - 16x_1 \\ \dot{x}_2 = 10x_2 - 6x_1 x_3 \\ \dot{x}_3 = 18x_2^2 - 5x_3 \end{cases}$	2.105	4
29	Wu et al. [53]	$\begin{cases} \dot{x}_1 = 6(x_2 - x_1) \\ \dot{x}_2 = 9x_1 - x_1 x_3 \\ \dot{x}_3 = x_1 x_2 - x_3 \end{cases}$	2.015	7
30	Bhalekar [54]	$\begin{cases} \dot{x}_1 = -x_2^2 - 2.667x_1 \\ \dot{x}_2 = 10(x_3 - x_1) \\ \dot{x}_3 = 27.3x_2 - x_3 + x_1 x_2 \end{cases}$	2.061	3
31	LR [55]	$\begin{cases} \dot{x}_1 = 19x_2 - 20x_1 - x_3 \\ \dot{x}_2 = 20x_1 + 8x_2 - 20x_1 x_3 \\ \dot{x}_3 = 5x_1 x_2 - 8.5x_3 + x_1(x_3 - 8) \end{cases}$	2.011	6
32	Su [56]	$\begin{cases} \dot{x}_1 = 5x_2 - 18x_1 \\ \dot{x}_2 = 10x_2 - 2x_1 x_3 \\ \dot{x}_3 = -x_3 + 5x_2^2 \end{cases}$	2.044	5
33	Akgul [57]	$\begin{cases} \dot{x}_1 = 1.8x_2 - 1.8x_1 \\ \dot{x}_2 = -7.2x_2 + x_1 x_3 + 0.02x_3 \\ \dot{x}_3 = 2.7x_3 + x_1^3 x_2 - 0.07x_3^2 \end{cases}$	2.024	5
34	Zhang [58]	$\begin{cases} \dot{x}_1 = -2x_1 + 10x_2 x_3 \\ \dot{x}_2 = -6x_2^3 + 3x_1 x_3 \\ \dot{x}_3 = 3x_3 - x_1 x_2 \end{cases}$	2.025	5
35	Gholamin et al. [59]	$\begin{cases} \dot{x}_1 = -4x_1 + 3x_2 x_3 \\ \dot{x}_2 = x_2 - 7x_1 x_3 \\ \dot{x}_3 = x_3 + 2x_1 x_2 \end{cases}$	2.055	6
36	Lai et al. [60]	$\begin{cases} \dot{x}_1 = 5(x_2 - x_1) \\ \dot{x}_2 = 2x_1 x_3(x_3^2 - 9) \\ \dot{x}_3 = 1 - x_1 x_2 \end{cases}$	2.196	6
37	Tuna et al. [61]	$\begin{cases} \dot{x}_1 = x_2(x_3 - 1.3) \\ \dot{x}_2 = -x_1(x_3 + 1.3) \\ \dot{x}_3 = -x_2(1.3x_1 - x_2) - 4(x_3 - 1.3) \end{cases}$	2.191	4

TABLE 3. *(Continued.)* Different reported chaotic systems with Kaplan-York dimension and bandwidth.

38	Vaidyanathan et al. [62]	$\begin{cases}\dot{x}_1 = 30(x_2 - x_1) + 14x_2x_3 \\ \dot{x}_2 = 14x_2 - x_1x_3^2 \\ \dot{x}_3 = x_1x_2 - 4.5x_3\end{cases}$	2.136	4
39	Volos et al. [63]	$\begin{cases}\dot{x}_1 = -x_2 \\ \dot{x}_2 = -x_3 \\ \dot{x}_3 = -0.7x_3 - x_1 + 0.00038\sinh(x_2)\end{cases}$	2.173	2.5
40	Jay et al. [64]	$\begin{cases}\dot{x}_1 = 32x_2 - 33x_1 - x_3 \\ \dot{x}_2 = 46.6x_1 + 12x_2 \pm 10x_1x_3 \\ \dot{x}_3 = \pm10x_1x_2 - 6x_3 + x_1(\pm x_3 - 11)\end{cases}$	2.16	13
41	Sambas et al. [65]	$\begin{cases}\dot{x}_1 = x_2x_3 \\ \dot{x}_2 = x_1\lvert x_3\rvert - x_2\lvert x_1\rvert \\ \dot{x}_3 = \lvert x_1\rvert - x_1^2\end{cases}$	2.072	1.5
42	Yang et al. [66]	$\begin{cases}\dot{x}_1 = x_2x_3 \\ \dot{x}_2 = x_1^2 - x_2 \\ \dot{x}_3 = 1 - 4x_1\end{cases}$	2.112	4
43	Lassoued et al. [67]	$\begin{cases}\dot{x}_1 = x_2 \\ \dot{x}_2 = x_3 \\ \dot{x}_3 = -x_3 - x_2 - 2.625x_1 + 0.25x_1\lvert x_1\rvert\end{cases}$	2.124	2
44	Vaidyanathan et al [68]	$\begin{cases}\dot{x}_1 = 3(x_2 - x_1) \\ \dot{x}_2 = x_1x_3 \\ \dot{x}_3 = 50 - x_1^4 - x_3\end{cases}$	2.162	9
45	Lien et al. [69]	$\begin{cases}\dot{x}_1 = -x_1 - 1.5x_2 + x_2x_3 \\ \dot{x}_2 = 2.5x_2 - x_1x_3 \\ \dot{x}_3 = -4.9x_3 + x_1x_2\end{cases}$	2.163	3
46	Kapitaniak et al. [70]	$\begin{cases}\dot{x}_1 = x_3 \\ \dot{x}_2 = -x_1 - x_3 \\ \dot{x}_3 = 0.1x_1 + 5x_2 - x_3 + x_1x_2 - 0.3x_1x_3 + 1\end{cases}$	2.107	3
47	Xu et al. [71]	$\begin{cases}\dot{x}_1 = x_3 \\ \dot{x}_2 = x_1^2 + x_2^2 - 4 \\ \dot{x}_3 = -4x_1 - x_1^2 + x_2^2\end{cases}$	2.047	2
48	Idowu et al. [72]	$\begin{cases}\dot{x}_1 = x_3 + (x_2 - 0.6)x_1 \\ \dot{x}_2 = 1 - 0.1x_2 - x_1^2 \\ \dot{x}_3 = -x_1 - x_3\end{cases}$	2.229	3
49	Jinjie et al [73]	$\begin{cases}\dot{x}_1 = -2x_1 + 10x_2 \\ \dot{x}_2 = 15x_1 - 2x_3 - x_1x_3 \\ \dot{x}_3 = x_1x_2 - x_3\end{cases}$	2.185	9

TABLE 3. *(Continued.)* Different reported chaotic systems with Kaplan-York dimension and bandwidth.

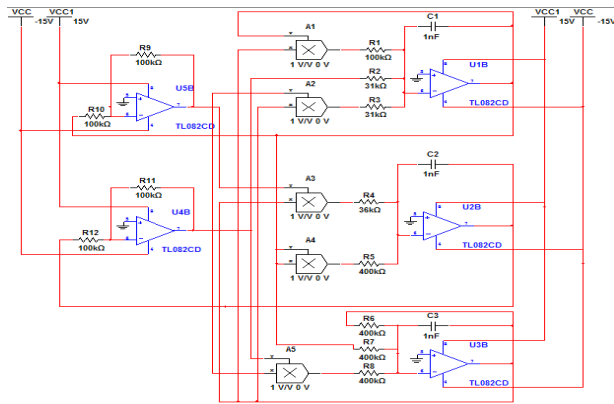| 50	Lai et al.[74]	$\begin{cases} \dot{x}_1 = 8(x_2 - x_1) \\ \dot{x}_2 = x_1 x_3 + e^{x_3} \\ \dot{x}_3 = 20 - x_1 x_2 \end{cases}$	2.091	8
51	System (1)	$\begin{cases} \dot{x}_1 = -ax_1 x_3 + bx_2(1 - x_3) \\ \dot{x}_2 = cx_1 x_3 - x_1^2 \\ \dot{x}_3 = -x_1 - x_3 + x_2^2 \end{cases}$	**2.281**	**15**

FIGURE 12. Electronic circuit schematic of the chaotic system (1).

FIGURE 13. Multisim result of the chaotic attractor, $x_1 - x_2$ plane.
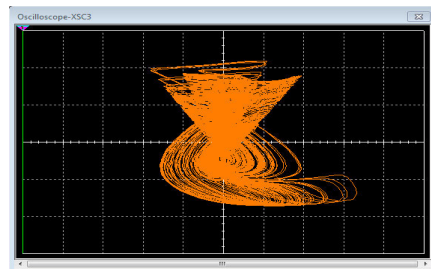
FIGURE 14. Multisim result of the chaotic attractor, $x_1 - x_3$ plane.

III. COMPARISON BETWEEN THE NEW CHAOTIC SYSTEM AND 50 REPORTED SYSTEMS

Based on many studies:

1- The Kaplan-York dimension (KYD) is a measure of a chaotic system's unpredictability and complexity. The higher the Kaplan-York dimension, the more complex the chaotic behaviour [23].

2- A chaotic system's carrier signal's bandwidth (BWT) should be big enough to cover the disguised information. In chaotic-based secure communications, large bandwidth is essential for achieving high data rate transmission [24]. In this section, a comparison between the Kaplan-York dimension and the bandwidth of the proposed chaotic system (1) with those of 50 reported chaotic systems is introduced. This comparison proved that the proposed model has a larger bandwidth and it is more complex when compare it to more than 50 considered systems, making it more helpful in a wide range of applications; especially in secure communication (see Table 2).

IV. CIRCUIT IMPLEMENTATION OF THE NEW SYSTEM

This section present an equivalent electronic circuit for our defined easy to use chaotic system (1), the electronic circuit is designed using Multisim software as depicted in Figure 12.
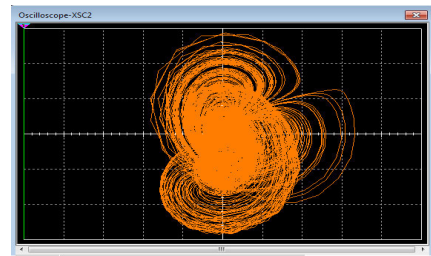
By affixing the law of Kirchhoff to Figure 12 circuit, it will generate nonlinear equations described as the following:

$$\begin{cases} \dot{x}_1 = -\dfrac{1}{C_1 R_1} x_1 x_3 - \dfrac{1}{C_1 R_2} x_2 x_3 + \dfrac{1}{C_1 R_3} x_2 \\ \dot{x}_2 = \dfrac{1}{C_2 R_4} x_1 x_3 - \dfrac{1}{C_2 R_5} x_1^2 \\ \dot{x}_3 = -\dfrac{1}{C_3 R_6} x_1 - \dfrac{1}{C_3 R_7} x_3 + \dfrac{1}{C_3 R_8} x_2^2 \end{cases} \quad (8)$$

The circuital components values are selected as:

$$R_1 = R_9 = R_{10} = R_{11} = R_{12} = 100k\Omega,$$
$$R_5 = R_6 = R_7 = R_8 = 400k\Omega$$
$$R_2 = R_3 = 31k\Omega, \quad R_4 = 36k\Omega,$$
$$C_1 = C_2 = C_3 = C_4 = 1nf \quad (9)$$

From Figures 13, 14 and 15 it can be seen the existence of the experiment chaotic attractors which are similar to the ones obtained by Matlab simulation. These results illustrate the physical feasibility of the proposed chaotic system (1).
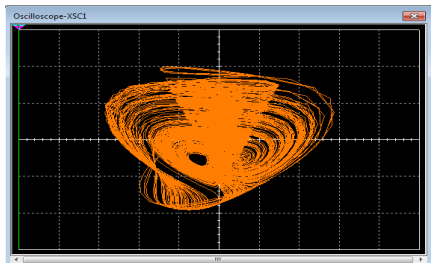
FIGURE 15. Multisim result of the chaotic attractor, $x_2 - x_3$ plane.

V. CONTROL AND SYNCHRONIZATION OF THE NEW CHAOTIC SYSTEM

A. DESIGN OF ACTIVE CONTROLLERS FOR CONTROLLING THE NEW CHAOTIC SYSTEM TO EQUILIBRIUM

In this subsection, an active control law is presented for control of the proposed chaotic system to one of its three points of equilibrium.

In order to control the proposed system to $E_1 = (0, 0, 0)$, active control functions are added to the new chaotic system. Then, the controlled system is considered as follows:

$$\begin{cases} \dot{x}_1 = -ax_1x_3 + bx_2(1 - x_3) + O_{x_1} \\ \dot{x}_2 = cx_1x_3 - x_1^2 + O_{x_2} \\ \dot{x}_3 = -x_1 - x_3 + x_2^2 + O_{x_3} \end{cases} \quad (10)$$

where O_{x_1}, O_{x_2} and O_{x_3} are the functions to be calculated for the active control, and the state errors are described by:

$$e_{x_1} = x_1 - x_{1d}, \quad e_{x_2} = x_2 - x_{2d}, \quad e_{x_3} = x_3 - x_{3d} \quad (11)$$

with

$$(x_{1d}, x_{2d}, x_{3d}) = (0, 0, 0) \quad (12)$$

By considering system (10) and the desired state (12), we obtained the following state errors dynamics:

$$\begin{cases} \dot{e}_{x_1} = \dot{x}_1 - \dot{x}_{1d} \\ \dot{e}_{x_2} = \dot{x}_2 - \dot{x}_{2d} \\ \dot{e}_{x_3} = \dot{x}_3 - \dot{x}_{3d} \end{cases}$$

So,

$$\begin{cases} \dot{e}_{x_1} = -ax_1x_3 - bx_2x_3 + be_{x_2} + O_{x_1} \\ \dot{e}_{x_2} = cx_1x_3 - x_1^2 + O_{x_2} \\ \dot{e}_{x_3} = x_2^2 - e_{x_1} - e_{x_3} + O_{x_3} \end{cases} \quad (13)$$

Theorem 1: Suppose the functions for the active control is chosen as follows:

$$\begin{cases} O_{x_1} = ax_1x_3 + bx_2x_3 - be_{x_2} - e_{x_1} \\ O_{x_2} = -cx_1x_3 + x_1^2 - e_{x_2} \\ O_{x_3} = -x_2^2 + e_{x_1} \end{cases} \quad (14)$$

Then, the state errors' dynamics is said to converge asymptotically to zero. Therefore, the controlled system (10) converges to the point of equilibrium $E_1 = (0, 0, 0)$.
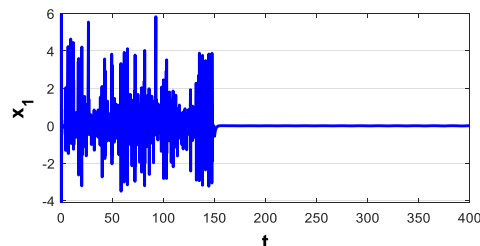

FIGURE 16. Time evolution of the new system first variable x_1 with controllers deactivated ($t < 150s$) and activated ($t \geq 150s$).
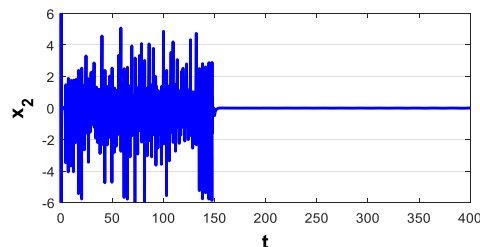

FIGURE 17. Time evolution of the new system second variable x_2 with controllers deactivated ($t < 150s$) and activated ($t \geq 150s$).
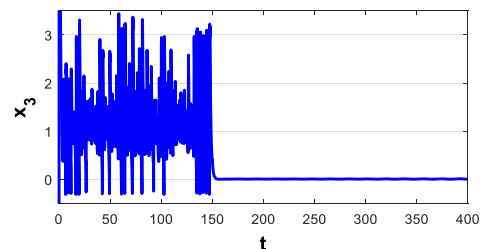

FIGURE 18. Time evolution of the new system third variable x_3 with controllers deactivated ($t < 150s$) and activated ($t \geq 150s$).

Proof: The state errors' dynamics (13) is re-written as follows, using the active control functions provided in (14):

$$\begin{cases} \dot{e}_{x_1} = -e_{x_1} \\ \dot{e}_{x_2} = -e_{x_2} \\ \dot{e}_{x_3} = -e_{x_3} \end{cases} \quad (15)$$

Therefore,

$$\begin{bmatrix} \dot{e}_{x_1} \\ \dot{e}_{x_2} \\ \dot{e}_{x_3} \end{bmatrix} = \begin{bmatrix} -1 & 0 & 0 \\ 0 & -1 & 0 \\ 0 & 0 & -1 \end{bmatrix} \begin{bmatrix} e_{x_1} \\ e_{x_1} \\ e_{x_3} \end{bmatrix} \quad (16)$$

Since the eigenvalues for the states matrix are negatives, then, based on Routh-Hurwitz condition [71]; the errors dynamics are stables, ensuring the convergence of the controlled new system (10) to equilibrium.

- *Simulation Results:*

System (10) initial conditions and parameters are chosen as $(x_1, x_2, x_3) = (1, 1, 1)$ and $a = 4$, $b = 13$ and $c = 11$ respectively. Active controllers is switched on at $t = 150s$. Simulation results are depicted in Figures 16, 17 and 18.

The results shows that all the three new system state variables generate a complex chaotic behaviour before

$t = 150s$ by deactivating the active controllers. After that (when $t \geq 150s$), the controllers are activated and it is obvious that all state variables converge quickly to zero (converge to the equilibrium point E_1).

So, results of simulation proving the efficiency of the new active controllers (14) for controlling the new chaotic system (1) to equilibrium.

B. DESIGN OF ACTIVE CONTROLLERS FOR TRACKING CONTROL OF THE NEW CHAOTIC SYSTEM

In this subsection, an active tracking control law is calculated for the proposed system for tracking any desired function of time $f(t)$.

For that, the controlled system is considered as follows:

$$\begin{cases} \dot{x}_1 = -ax_1x_3 + bx_2(1-x_3) + P_{x_1} \\ \dot{x}_2 = cx_1x_3 - x_1^2 + P_{x_2} \\ \dot{x}_3 = -x_1 - x_3 + x_2^2 + P_{x_3} \end{cases} \quad (17)$$

where P_{x_1}, P_{x_2} and P_{x_3} is the functions for the active trailing control to be obtained, and the state errors are described by:

$$e_{x_1} = x_1 - x_{1d}, \quad e_{x_2} = x_2 - x_{2d}, \quad e_{x_3} = x_3 - x_{3d} \quad (18)$$

with

$$(x_{1d}, \ x_{2d}, \ x_{3d}) = (f(t), \ f(t), \ f(t)) \quad (19)$$

By considering system (17) and the desired state (19), we obtained the following state errors dynamics:

$$\begin{cases} \dot{e}_{x_1} = \dot{x}_1 - \dot{f}(t) \\ \dot{e}_{x_2} = \dot{x}_2 - \dot{f}(t) \\ \dot{e}_{x_3} = \dot{x}_3 - \dot{f}(t) \end{cases}$$

So,

$$\begin{cases} \dot{e}_{x_1} = -ax_1x_3 - bx_2(1-x_3) - \dot{f}(t) + P_{x_1} \\ \dot{e}_{x_2} = cx_1x_3 - x_1^2 - \dot{f}(t) + P_{x_2} \\ \dot{e}_{x_3} = -x_1 - x_3 + x_2^2 - \dot{f}(t) + P_{x_3} \end{cases} \quad (20)$$

Theorem 2: Suppose the functions for the active tracking control is chosen as:

$$\begin{cases} P_{x_1} = ax_1x_3 + bx_2x_3 - bx_2 - x_1 + \dot{f}(t) \\ P_{x_2} = -cx_1x_3 + x_1^2 - x_2 + \dot{f}(t) \\ P_{x_3} = x_1 - x_2^2 + \dot{f}(t) \end{cases} \quad (21)$$

The dynamical of state errors will be converge asymptotically to zero. Therefore, system (17) is controlled to track any desired function of time $f(t)$.

Proof: The dynamics of state errors (20) can be recast using the active control tracking functions provided in (21), as follows:

$$\begin{cases} \dot{e}_{x_1} = -e_{x_1} \\ \dot{e}_{x_2} = -e_{x_2} \\ \dot{e}_{x_3} = -e_{x_3} \end{cases} \quad (22)$$

Therefore,

$$\begin{bmatrix} \dot{e}_{x_1} \\ \dot{e}_{x_2} \\ \dot{e}_{x_3} \end{bmatrix} = \begin{bmatrix} -1 & 0 & 0 \\ 0 & -1 & 0 \\ 0 & 0 & -1 \end{bmatrix} \begin{bmatrix} e_{x_1} \\ e_{x_1} \\ e_{x_3} \end{bmatrix} \quad (23)$$

Because all of the state matrix's eigenvalues are negative, the errors dynamics are stable, ensuring that the controlled new system (17) converges to the function $f(t)$ according to the Routh-Hurwitz criterion [71].

- *Simulation Results:*

System (17) initial conditions and parameters are given as $(x_1, x_2, x_3) = (1, 1, 1)$ and $a = 4$, $b = 13$ and $c = 11$ respectively. The function of time $f(t)$ is chosen as $f(t) = 4\sin(0.5t)$. Active tracking controllers is switched on at $t = 150s$, simulation results are depicted in Figures 19, 20 and 21.

The results shows that all the three new system state variables generate a complex chaotic behaviour when the active controllers are deactivated (when $t < 150s$). After that (when $t \geq 150s$), the controllers are activated and it can be seen that all state variables switch quickly to exhibit a sine wave behaviour and to track the sine function $f(t) = 4\sin(0.5t)$.

So, simulation findings proving the success of the suggested active tracking controllers (21) for controlling the new chaotic system (1) in tracking any desired function of time including $f(t) = 4\sin(0.5t)$.

C. DESIGN OF ACTIVE CONTROLLERS FOR SYNCHRONIZING THE PROPOSED CHAOTIC SYSTEM

In this subsection, we use active control to synchronise two identical new chaotic systems (1) with differing initial values.

The master system is demonstrated as the following:

$$\begin{cases} \dot{x}_{1m} = -ax_{1m}x_{3m} + bx_{2m}(1-x_{3m}) \\ \dot{x}_{2m} = cx_{1m}x_{3m} - x_{1m}^2 \\ \dot{x}_{3m} = -x_{1m} - x_{3m} + x_{2m}^2 \end{cases} \quad (24)$$

The, the slave system is described as:

$$\begin{cases} \dot{x}_{1s} = -ax_{1s}x_{3s} + bx_{2s}(1-x_{3s}) + Q_{x_1} \\ \dot{x}_{2s} = cx_{1s}x_{3s} - x_{1s}^2 + Q_{x_2} \\ \dot{x}_{3s} = -x_{1s} - x_{3s} + x_{2s}^2 + Q_{x_3} \end{cases} \quad (25)$$

where functions of active control represented by Q_{x_1}, Q_{x_2} and Q_{x_3} are to obtained, and the state errors are described by:

$$e_{x_1} = x_{1s} - x_{1m}, \quad e_{x_2} = x_{2s} - x_{2m}, \quad e_{x_3} = x_{3s} - x_{3m} \quad (26)$$

By considering systems (24), (25) and (26), the dynamic state errors is obtained:

$$\begin{cases} \dot{e}_{x_1} = a(x_{1m}x_{3m} - x_{1s}x_{3s}) + b(x_{2m}x_{3m} - x_{2s}x_{3s}) + be_{x_2} \\ \quad + Q_{x_1} \\ \dot{e}_{x_2} = c(x_{1s}x_{3s} - x_{1m}x_{3m}) - (x_{1s}^2 - x_{1m}^2) + Q_{x_2} \\ \dot{e}_{x_3} = -e_{x_3} - e_{x_1} + x_{2s}^2 - x_{2m}^2 + Q_{x_3} \end{cases}$$
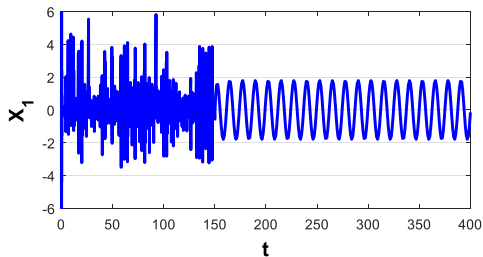
$$(27)$$

FIGURE 19. Time evolution of the new system first state x_1 with tracking controllers deactivated ($t < 150s$) and activated ($t \geq 150s$).
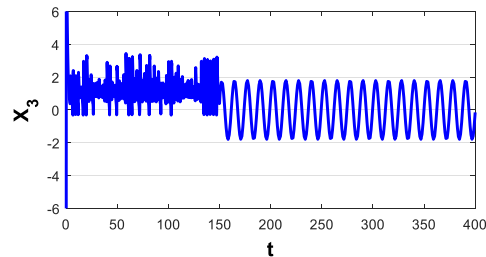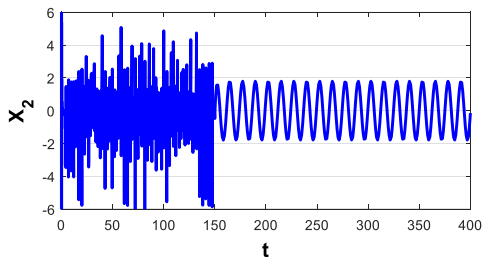

FIGURE 20. Time evolution of the new system second state x_2 with tracking controllers deactivated ($t < 150s$) and activated ($t \geq 150s$).
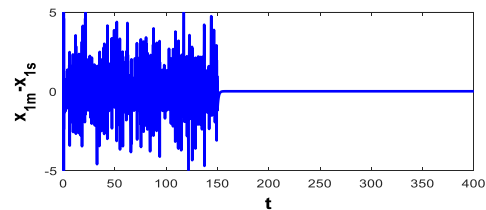

FIGURE 21. Time evolution of the new system third state x_3 with tracking controllers deactivated ($t < 150s$) and activated ($t \geq 150s$).

FIGURE 22. Time evolution of the first state synchronization error with controllers deactivated ($t < 150s$) and activated ($t \geq 150s$).
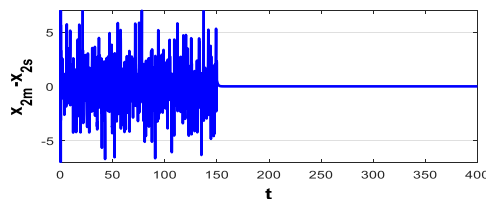

FIGURE 23. Time evolution of the second state synchronization error with controllers deactivated ($t < 150s$) and activated ($t \geq 150s$).
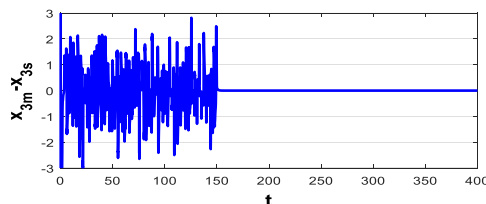

FIGURE 24. Time evolution of the third state synchronization error with controllers deactivated ($t < 150s$) and activated ($t \geq 150s$).

Theorem 3: Suppose the active control functions is chosen as follows:

$$\begin{cases} Q_{x_1} = -a(x_{1m}x_{3m} - x_{1s}x_{3s}) - b(x_{2m}x_{3m} - x_{2s}x_{3s}) - be_{x_2} \\ \quad - e_{x_1} \\ Q_{x_2} = -c(x_{1s}x_{3s} - x_{1m}x_{3m}) + (x_{1s}^2 - x_{1m}^2) - e_{x_2} \\ Q_{x_3} = -x_{2s}^2 + x_{2m}^2 + e_{x_1} \end{cases}$$
$$(28)$$

Then, the dynamical state errors will asymptotically converge to zero. As a result, the master (24) and slave (25) systems will be synced.

Proof: The dynamics of state errors (27) can be simplified using the active control functions given in (28).

$$\begin{cases} \dot{e}_{x_1} = -e_{x_1} \\ \dot{e}_{x_2} = -e_{x_2} \\ \dot{e}_{x_3} = -e_{x_3} \end{cases}$$
$$(29)$$

Therefore,

$$\begin{bmatrix} \dot{e}_{x_1} \\ \dot{e}_{x_2} \\ \dot{e}_{x_3} \end{bmatrix} = \begin{bmatrix} -1 & 0 & 0 \\ 0 & -1 & 0 \\ 0 & 0 & -1 \end{bmatrix} \begin{bmatrix} e_{x_1} \\ e_{x_1} \\ e_{x_3} \end{bmatrix}$$
$$(30)$$

Because all of the states matrix's eigenvalues are negative, the error dynamics are stable, ensuring synchronisation between the master and slave systems (24) according to the Routh-Hurwitz criterion [71].

- *Simulation Results:*

The master and slave systems' initial conditions defined in (24) and (25) are selected as (1, 1, 1) and (−5, 7, −15) respectively.

Active controllers is switched on at $t = 150s$, simulation results are depicted in Figures 22, 23 and 24.

The results shows that all the three state synchronization errors evolve chaotically with time by deactivating the active controllers (when $t < 150s$). After that (when $t \geq 150s$), the controllers are activated, then, the convergence all the state synchronization errors to zero is very obvious.

So, simulation findings showing the feat of the new active controllers (28) to synchronize two new identical chaotic systems (1) starting from various initial guesses.

VI. SECURE COMMUNICATION CIRCUIT DESIGN BASED ON THE NEW CHAOTIC SYSTEM
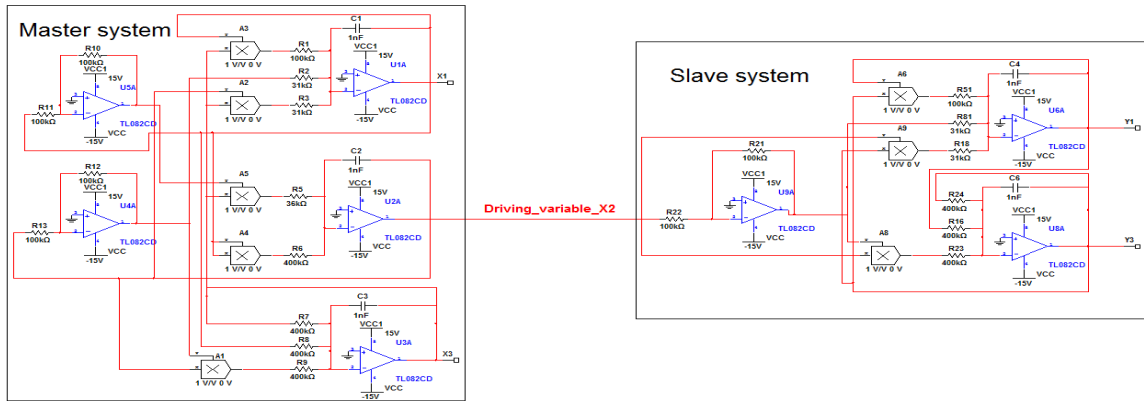To demonstrate the applicability of the proposed system (1) in securing communications, we create a new secure

FIGURE 25. Circuit schematic of the drive response synchronization.

communication circuit schematic centered around the proposed system and employing drive response synchronization, with the use of a single state variable to attain strong self-synchronization.

A. DRIVE RESPONSE SYNCHRONIZATION

In this subsection, we present the synchronization electronic circuit schematic of two identical new chaotic systems (1) starting from different initial values using drive response method. We use the proposed system (1) as a master system, also as a slave system. The driving variable generated by the master system ensures the synchronization of states of the master system and the states of the slave system.

The slave system presented below is described by considering the proposed eight terms chaotic system (1) as a master system:

$$\begin{cases} \dot{y}_1 = -ay_1y_3 + by_2(1 - y_3) \\ \dot{y}_2 = cy_1y_3 - y_1^2 \\ \dot{y}_3 = -y_1 - y_3 + y_2^2 \end{cases} \quad (31)$$

By selecting the master system's second state variable of the x_2 as the driving variable, the slave system become as the following:

$$\begin{cases} \dot{y}_1 = -ay_1y_3 + bx_2(1 - y_3) \\ \dot{y}_3 = -y_1 - y_3 + x_2^2 \end{cases} \quad (32)$$

Electronic circuit schematic of the drive response synchronization between master system and slave system is depicted in Figure 25.

The initial condition of system (1) and (32) are chosen as (1, 1, 1) and (−5, −10) respectively. Time evolutions of the first states (x_1 and y_1) are depicted in Figure 26; Figure 27 shows the time evolution of the third states (x_3 and y_3).

The drive response approach was successful in synchronizing the two identical master and slave chaotic systems starting from differing initial circumstances, as shown in simulation results in Figures 26 and 27.

FIGURE 26. Time evolution of master system first state x_1 (red color) and slave system first state y_1 (blue color).
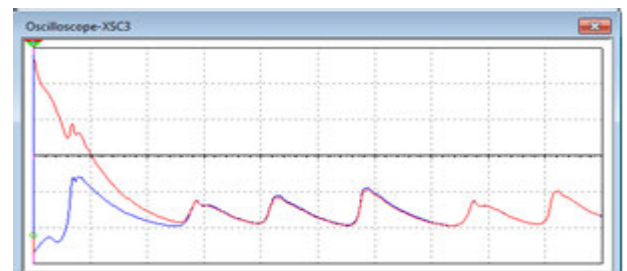

FIGURE 27. Time evolution of master system third state x_3 (red color) and slave system third state y_3 (blue color).

Remark: All values of the circuitals components are mentioned in the previous figures

B. SECURE COMMUNICATION CIRCUIT IMPLEMENTATION

In this subsection, a secure communication electronic circuit schematic is designed using the new eight terms chaotic system (1) and based on the drive response synchronization. Then, its experiment simulation results are obtained using Multisim software.

Figure 28 shows the electronic circuit design for the secure communication strategy created for the new chaotic system. We can see that two signals are transmitted from the transmitter to the receiver, the first one is the driving variable x_2 so as to complete synchronization between the master system
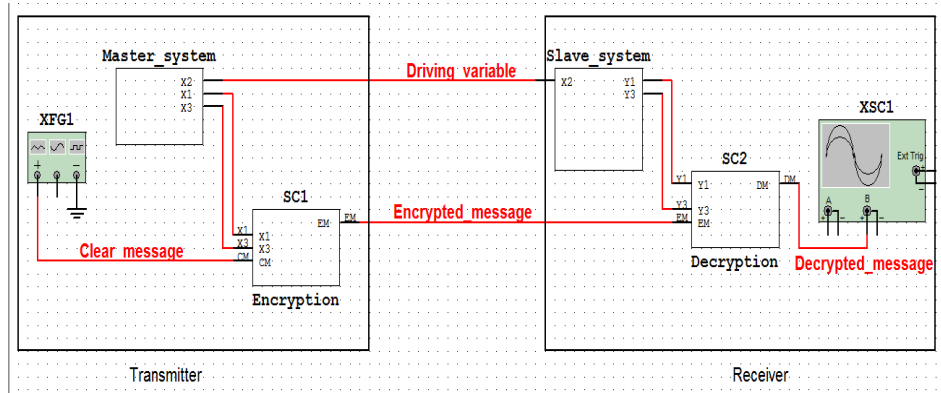
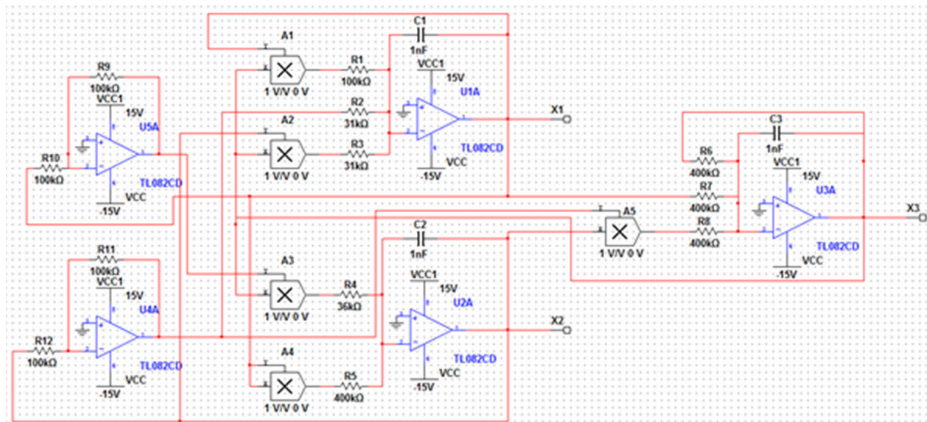**FIGURE 28.** Electronic circuit of the secure communication scheme.

FIGURE 29. Electronic circuit schematic of the master system.
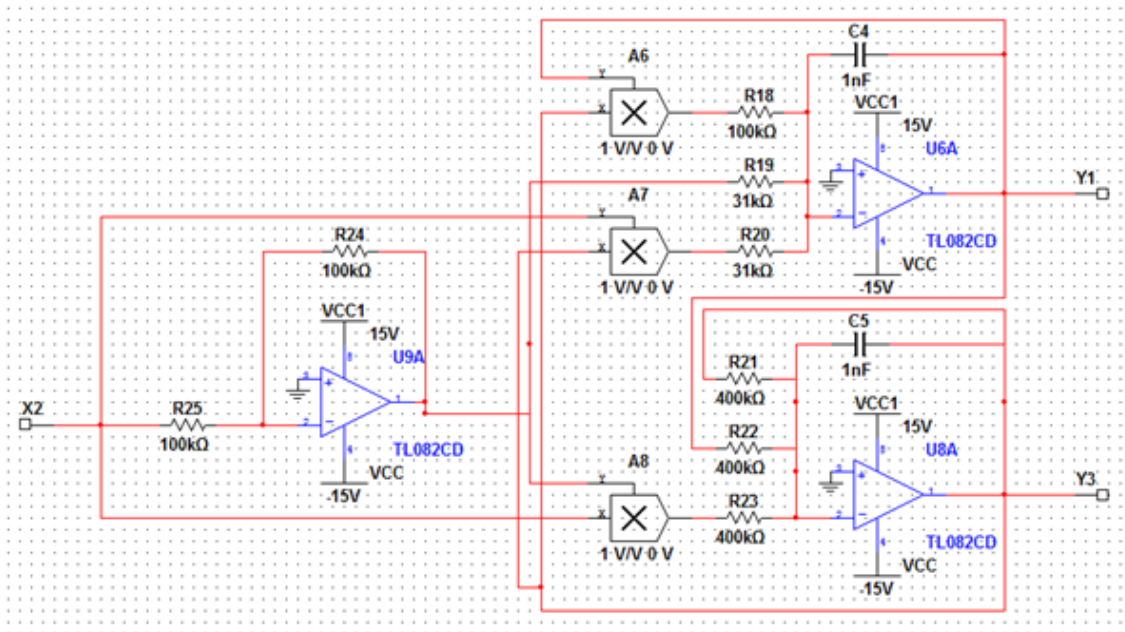

FIGURE 30. Electronic circuit schematic of the slave system.

and the slave system, the second signal transmitted is the encrypted message $\widehat{m}$.

The encrypted message $\widehat{m}$ is obtained using the electronic circuit schematic depicted in Figure 31 based on the linear
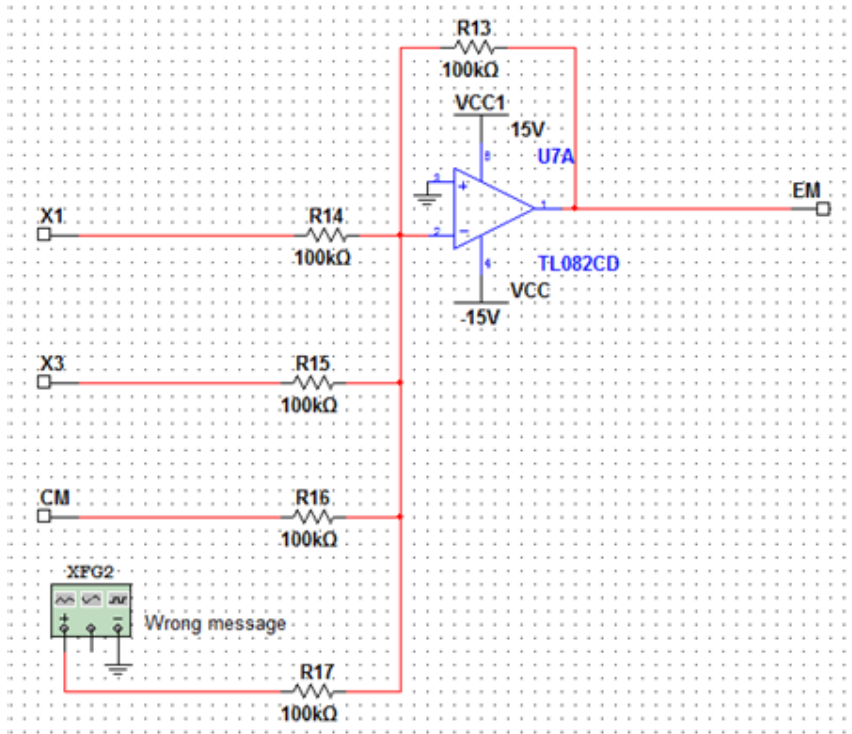
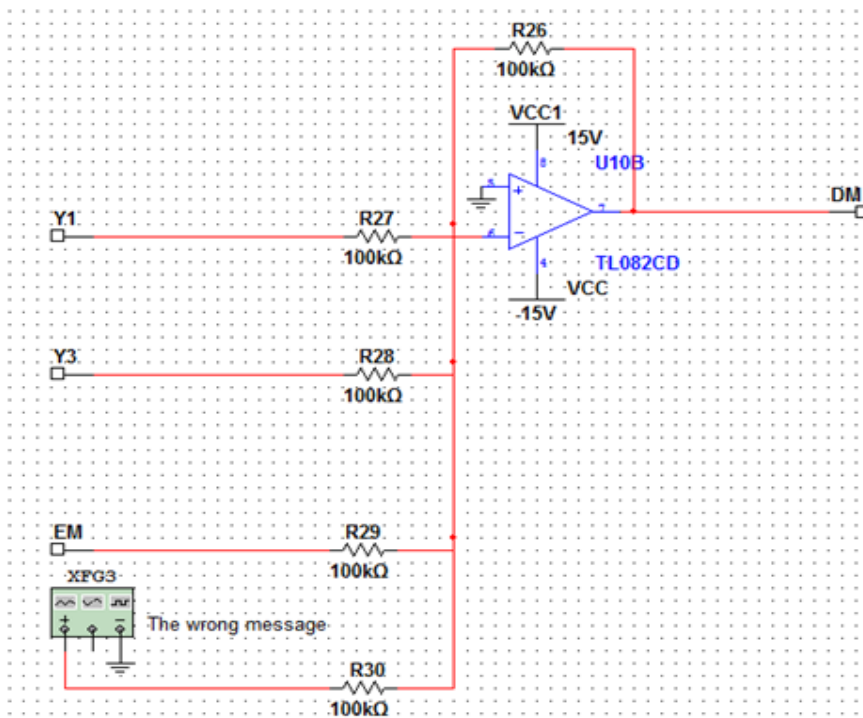**FIGURE 31.** Electronic circuit schematic of the encryption process.

FIGURE 32. Electronic circuit schematic of the decryption process.

equation define below:

$$\widehat{m} = -(k_1 \times m + k_2 \times w + k_3 \times x_1 + k_4 \times x_3) \quad (33)$$

where x_1, x_3 represent the master system's state variables, m is the clear message, w is a wrong message assumed to be

known which is included to increase the complexity of the encrypted message; k_1, k_2, k_3, k_4 are parameters (constant) used as an additional transmission secret key.

When the synchronization is achieved, the decrypted message $\bar{m}$ is reconstructed in the receiver using the electronic
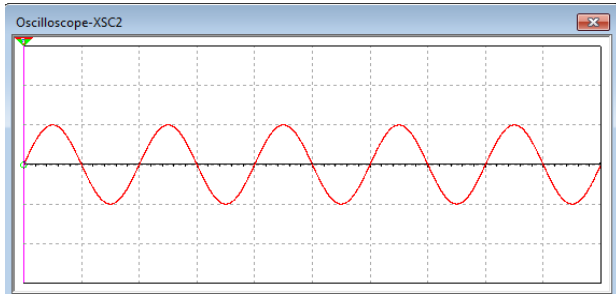
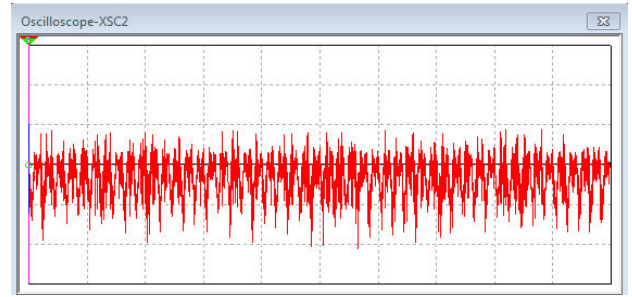**FIGURE 33.** Time evolution of the clear message (case 1).

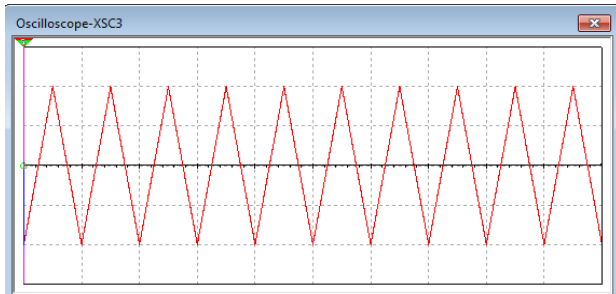**FIGURE 35.** Time evolution of the encrypted message (case 1).

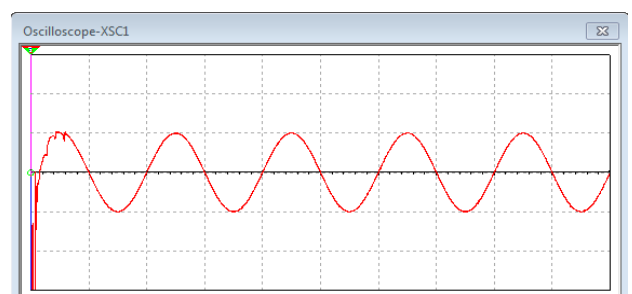**FIGURE 34.** Time evolution of the wrong message (case 1).

FIGURE 36. Time evolution of the decrypted message (case 1).

circuit schematic depicted in Figure 32 based on the linear equation defined below:

$$\bar{m} = -\frac{1}{k_1}\left(\widehat{m} + k_2 \times w + k_3 \times y_1 + k_4 \times y_3\right), \quad k_1 \neq 0 \tag{34}$$

where y_1, y_3 representing the slave system's state variables, $\widehat{m}$ is the encrypted message and w is the same wrong message as in the transmitter.

For computational simulation:

We used the following constant parameters for the encryption and decryption functions:

$$k_1 = k_2 = k_3 = k_4 = 1 \tag{35}$$

Case 1: the sine wave is chosen as the clear message to be communicated as shown in Figure 33 and the triangle wave as the wrong message to be included in the encryption and decryption functions as shown in Figure 34. Figure 35 depicts the encrypted message's complicated chaotic behaviour, demonstrating the effectiveness of the encrypting process in concealing the clear information. The decrypted message is shown in Figure 36, and it is identical to the clear message. Figure 37 depicts the convergence of the message reconstruction error to zero after synchronisation, indicating that the decryption procedure was successful in reconstructing the original message.

Case 2: The triangle wave is used as the clear message to be transmitted, while the sine wave is used as the wrong message in the encryption and decryption processes. Clear message, wrong message, encrypted message, decrypted

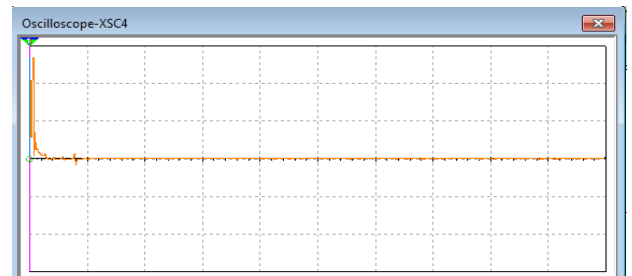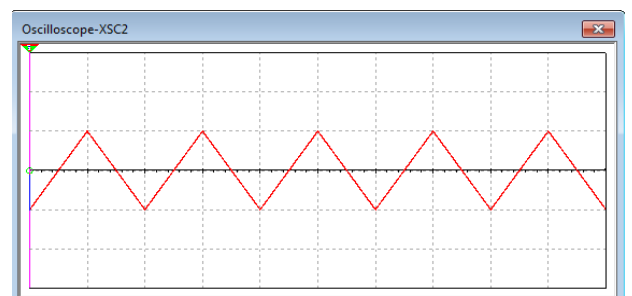**FIGURE 37.** Message reconstruction error (case 1).

FIGURE 38. Time evolution of the clear message (case 2).

message and message reconstruction error are ploted in Figures 38, 39, 40, 41 and 42 respectively.

The proposed secure communication electronic circuit schematic based on the novel eight terms chaotic system (1) was shown to be successful in completing the secure transmission/reception procedure.
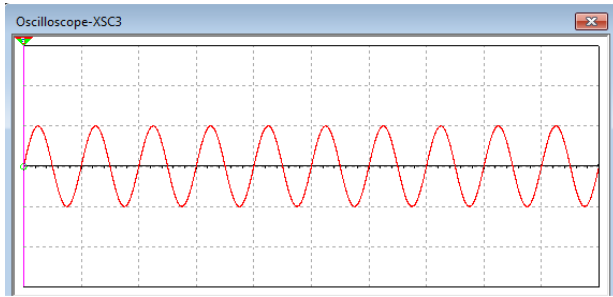
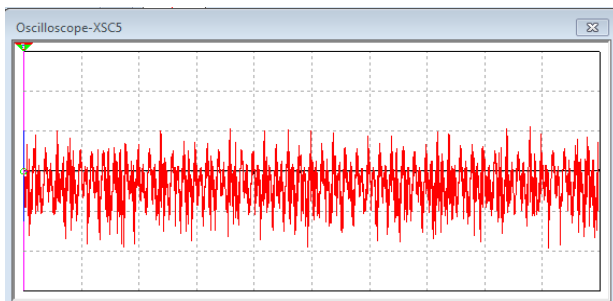**FIGURE 39.** Time evolution of the wrong message (case 2).

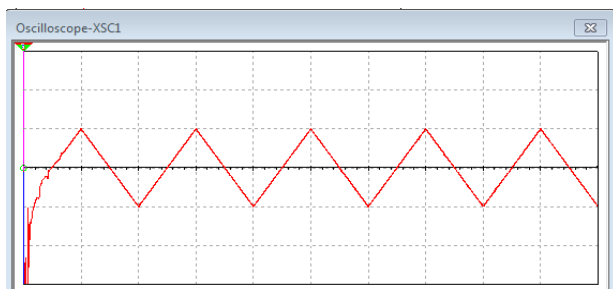**FIGURE 40.** Time evolution of the encrypted message (case 2).

FIGURE 41. Time evolution of the decrypted message (case 2).
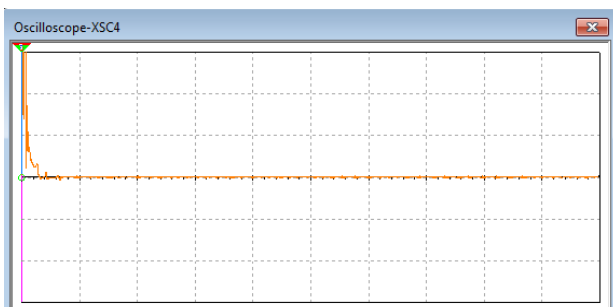

FIGURE 42. Message reconstruction error (case 2).

VII. CONCLUSION

This paper suggested a new three-dimensional eight terms chaotic system with five quadratic nonlinearities for the first time. The new system is more complicated and has a wider bandwidth than at least 50 other chaotic systems studied recently. Dynamical analysis of the new system are

widely studied via many tools which include: phase portraits, equilibrium points, dissipativity, multistability, bifurcation diagram and Lyapunov exponents spectrum. The physical feasibility of our proposed theoretical model is proved by using Multisim software to design the equivalent electronic circuit. After that, control of the proposed chaotic system for achieving stability, tracking and synchronization is studied and applied using active controllers, the obtained results illustrate the effectiveness of the suggested control laws. Finally, employing drive response synchronization, a new secure communication electronic circuit schematic is derived for the new chaotic system. Multisim simulation findings show that the proposed circuit schematic completed the secure transmission/reception process successfully.

We are convinced that the new 3D chaotic system with its easy to implement secure communication electronic circuit schematic, multistability and large bandwidth would be useful in the near future for real-world secure transmission systems.

REFERENCES

[1] E. N. Lorenz, "Deterministic nonperiodic flow," *J. Atmos. Sci.*, vol. 20, no. 2, pp. 130–141, Mar. 1963.

[2] A. Sambas, S. Vaidyanathan, E. Tlelo-Cuautle, B. Abd-El-Atty, A. A. A. El-Latif, O. Guille-Fernandez, Sukono, Y. Hidayat, and G. Gundara, "A 3-D multi-stable system with a peanut-shaped equilibrium curve: Circuit design, FPGA realization, and an application to image encryption," *IEEE Access*, vol. 8, pp. 137116–137132, 2020. [Online]. Available: https://ieeexplore.ieee.org/document/9146866/authors

[3] A. Sambas, M. Mamat, A. A. Arafa, G. M. Mahmoud, M. A. Mohamed, and W. S. Sanjaya, "A new chaotic system with line of equilibria: Dynamics, passive control and circuit design," *Int. J. Electr. Comput. Eng.*, vol. 9, no. 4, pp. 2365–2376, 2019.

[4] S. Mobayen, S. T. Kingni, V.-T. Pham, F. Nazarimehr, and S. Jafari, "Analysis, synchronisation and circuit design of a new highly nonlinear chaotic system," *Int. J. Syst. Sci.*, vol. 49, no. 3, pp. 617–630, Feb. 2018.

[5] A. Sambas, S. Vaidyanathan, S. Zhang, Y. Zeng, M. A. Mohamed, and M. Mamat, "A new double-wing chaotic system with coexisting attractors and line equilibrium: Bifurcation analysis and electronic circuit simulation," *IEEE Access*, vol. 7, pp. 115454–115462, 2019.

[6] A. Sambas, S. Vaidyanathan, T. Bonny, S. Zhang, Sukono, Y. Hidayat, G. Gundara, and M. Mamat, "Mathematical model and FPGA realization of a multi-stable chaotic dynamical system with a closed butterfly-like curve of equilibrium points," *Appl. Sci.*, vol. 11, no. 2, p. 788, Jan. 2021.

[7] V. T. Pham, T. Kapitaniak, S. Jafari, and X. Wang, "Dynamics and circuit of a chaotic system with a curve of equilibrium points," *Int. J. Electron.*, vol. 105, no. 3, pp. 385–397, 2018.

[8] A. Akgul, S. Hussain, and İ. Pehlivan, "A new three-dimensional chaotic system, its dynamical analysis and electronic circuit applications," *Optik*, vol. 127, no. 18, pp. 7062–7071, 2016.

[9] H.-P. Ren, H.-P. Yin, C. Bai, and J.-L. Yao, "Performance improvement of chaotic baseband wireless communication using echo state network," *IEEE Trans. Commun.*, vol. 68, no. 10, pp. 6525–6536, Oct. 2020.

[10] J. Wang, W. Yu, J. Wang, Y. Zhao, J. Zhang, and D. Jiang, "A new six-dimensional hyperchaotic system and its secure communication circuit implementation," *Int. J. Circuit Theory Appl.*, vol. 47, no. 5, pp. 702–717, May 2019.

[11] K. Benkouider, M. Halimi, and T. Bouden, "Secure communication scheme using chaotic time-varying delayed system," *Int. J. Comput. Appl. Technol.*, vol. 60, no. 2, pp. 175–182, 2019.

[12] P. Nagy and P. Tasnádi, "Visualization of chaotic attractors in 3D as motivating tool for introductory physics course," *J. Phys., Conf. Ser.*, vol. 1286, Aug. 2019, Art. no. 012028.

[13] S. Vaidyanathan, A. Sambas, M. Mamat, and W. M. Sanjaya, "A new three-dimensional chaotic system with a hidden attractor, circuit design and application in wireless mobile robot," *Arch. Control Sci.*, vol. 27, no. 4, pp. 541–554, 2017.

[14] T. Asano and M. Yokoo, "Chaotic dynamics of a piecewise linear model of credit cycles," *J. Math. Econ.*, vol. 80, pp. 9–21, Jan. 2019.

[15] M. J. Wishon, N. Li, D. Choi, D. S. Citrin, and A. Locquet, "Chaotic laser voltage: An electronic entropy source," *Appl. Phys. Lett.*, vol. 112, no. 26, Jun. 2018, Art. no. 261101.

[16] C. Villacorta-Rath, C. A. Souza, N. P. Murphy, B. S. Green, C. Gardner, and J. M. Strugnell, "Temporal genetic patterns of diversity and structure evidence chaotic genetic patchiness in a spiny lobster," *Mol. Ecol.*, vol. 27, no. 1, pp. 54–65, Jan. 2018.

[17] T. L. Carroll and L. M. Pecora, "Synchronizing chaotic circuits," *IEEE Trans. Circuits Syst.*, vol. 38, no. 4, pp. 453–456, Apr. 1991.

[18] A. Sambas, S. Vaidyanathan, I. Moroz, B. Idowu, M. Mohamed, M. Mamat, and W. Sanjaya, "A simple multi-stable chaotic jerk system with two saddle-foci equilibrium points: Analysis, synchronization via backstepping technique and MultiSim circuit design," *Int. J. Electr. Comput. Eng.*, vol. 11, no. 4, pp. 2941–2952, 2021.

[19] S. Kumar, A. E. Matouk, H. Chaudhary, and S. Kant, "Control and synchronization of fractional–order chaotic satellite systems using feedback and adaptive control techniques," *Int. J. Adapt. Control Signal Process.*, vol. 35, no. 4, pp. 484–497, Apr. 2021.

[20] S. Vaidyanathan, "Analysis and adaptive control of a novel 3-D conservative no-equilibrium chaotic system," *Arch. Control Sci.*, vol. 25, no. 3, pp. 1–21, 2015.

[21] K. Benkouider, T. Bouden, and M. Halimi, "Dynamical analysis, synchronization and circuit implementation of a new hyperchaotic system with line equilibrium," in *Proc. 6th Int. Conf. Control, Decis. Inf. Technol. (CoDIT)*, Apr. 2019, pp. 1717–1722.

[22] R. Kharel, "Design and implementation of secure chaotic communication systems," Ph.D. dissertation, School Comput., Eng. Inf. Sci., Northumbria Univ., Newcastle, U.K., 2011.

[23] P. Frederickson, J. L. Kaplan, E. D. Yorke, and J. A. Yorke, "The Liapunov dimension of strange attractors," *J. Differ. Equ.*, vol. 49, no. 2, pp. 185–207, 1983.

[24] G. Qi, G. Chen, and Y. Zhang, "On a new asymmetric chaotic system," *Chaos, Solitons Fractals*, vol. 37, no. 2, pp. 409–423, Jul. 2008.

[25] G. Chen and T. Ueta, "Yet another chaotic attractor," *Int. J. Bifurcation Chaos*, vol. 9, no. 7, pp. 1465–1466, 1999.

[26] O. E. Rössler, "An equation for continuous chaos," *Phys. Lett. A*, vol. 57, no. 5, pp. 397–398, 1976.

[27] Z. Chen, Y. Yang, and Z. Yuan, "A single three-wing or four-wing chaotic attractor generated from a three-dimensional smooth quadratic autonomous system," *Chaos, Solitons Fractals*, vol. 38, no. 4, pp. 1187–1196, Nov. 2008.

[28] D. Li, "A three-scroll chaotic attractor," *Phys. Lett. A*, vol. 372, no. 4, pp. 387–393, Jan. 2008.

[29] W. Zhou, Y. Xu, H. Lu, and L. Pan, "On dynamics analysis of a new chaotic attractor," *Phys. Lett. A*, vol. 372, no. 36, pp. 5773–5777, Sep. 2008.

[30] J. Lü, D. Cheng, S. Celikovsky, and G. Chen, "Bridge the gap between the Lorenz system and the Chen system," *Int. J. Bifurcation Chaos*, vol. 12, pp. 2917–2926, Dec. 2002.

[31] C. Sparrow, *The Lorenz Equations: Bifurcations, Chaos, and Strange Attractors*, vol. 41. New York, NY, USA: Springer, 2012.

[32] G. Cai and Z. Tan, "Chaos synchronization of a new chaotic system via nonlinear control," *J. Uncertain Syst.*, vol. 1, no. 3, pp. 235–240, 2007.

[33] G. Tigan and D. Opriş, "Analysis of a 3D chaotic system," *Chaos, Solitons Fractals*, vol. 36, no. 5, pp. 1315–1319, Jun. 2008.

[34] G. Wang, X. Zhang, Y. Zheng, and Y. Li, "A new modified hyperchaotic Lü system," *Phys. A, Stat. Mech. Appl.*, vol. 371, no. 2, pp. 260–272, 2006.

[35] C. Liu, T. Liu, L. Liu, and K. Liu, "A new chaotic attractor," *Chaos, Solitons Fractals*, vol. 22, no. 5, pp. 1031–1038, Dec. 2004.

[36] X.-F. Li, Y.-D. Chu, J.-G. Zhang, and Y.-X. Chang, "Nonlinear dynamics and circuit implementation for a new lorenz-like attractor," *Chaos, Solitons Fractals*, vol. 41, no. 5, pp. 2360–2370, Sep. 2009.

[37] B. Munmuangsaen and B. Srisuchinwong, "A new five-term simple chaotic attractor," *Phys. Lett. A*, vol. 373, no. 44, pp. 4038–4043, Oct. 2009.

[38] Y. Liu and Q. Yang, "Dynamics of a new Lorenz-like chaotic system," *Nonlinear Anal., Real World Appl.*, vol. 11, pp. 2563–2572, Aug. 2010.

[39] C. X. Zhu, Y. H. Liu, and Y. Guo, "Theoretic and numerical study of a new chaotic system," *Intell. Inf. Manage.*, vol. 2, no. 2, pp. 104–109, 2010.

[40] L. Pan, W. Zhou, J. A. Fang, and D. Li, "A new three-scroll unified chaotic system coined," *Int. J. Nonlinear Sci.*, vol. 10, no. 4, pp. 462–474 2010.

[41] I. Pehlivan and Y. U. Lu, "A new chaotic attractor from general Lorenz system family and its electronic experimental implementation," *Turkish J. Elect. Eng. Comput. Sci.*, vol. 18, no. 2, pp. 171–184, 2010.

[42] Z. Wei, "Dynamical behaviors of a chaotic system with no equilibria," *Phys. Lett. A*, vol. 376, no. 2, pp. 102–108, Dec. 2011.

[43] X. Li and Q. Ou, "Dynamical properties and simulation of a new lorenz-like chaotic system," *Nonlinear Dyn.*, vol. 65, no. 3, pp. 255–270, Aug. 2011.

[44] C. Li, H. Li, and Y. Tong, "Analysis of a novel three-dimensional chaotic system," *Optik*, vol. 124, no. 13, pp. 1516–1522, Jul. 2013.

[45] D. Kim and P. H. Chang, "A new butterfly-shaped chaotic attractor," *Results Phys.*, vol. 3, pp. 14–19, 2013.

[46] A. Abooee, H. A. Yaghini-Bonabi, and M. R. Jahed-Motlagh, "Analysis and circuitry realization of a novel three-dimensional chaotic system," *Commun. Nonlinear Sci. Numer. Simul.*, vol. 18, no. 5, pp. 1235–1245, May 2013.

[47] Z. Qiao and X. Li, "Dynamical analysis and numerical simulation of a new lorenz-type chaotic system," *Math. Comput. Model. Dyn. Syst.*, vol. 20, no. 3, pp. 264–283, May 2014.

[48] K. Deng, J. Li, and S. Yu, "Dynamics analysis and synchronization of a new chaotic attractor," *Optik*, vol. 125, no. 13, pp. 3071–3075, Jul. 2014.

[49] A. Gholizadeh, H. S. Nik, and A. Jajarmi, "Analysis and control of a three-dimensional autonomous chaotic system," *Appl. Math. Inf. Sci.*, vol. 9, pp. 739–747, 2015.

[50] X. Wu, Y. He, W. Yu, and B. Yin, "A new chaotic attractor and its synchronization implementation," *Circuits, Syst., Signal Process.*, vol. 34, no. 6, pp. 1747–1768, Jun. 2015.

[51] P. P. Singh, J. P. Singh, and B. K. Roy, "Synchronization and anti-synchronization of lu and Bhalekar–Gejji chaotic systems using nonlinear active control," *Chaos, Solitons Fractals*, vol. 69, pp. 31–39, Dec. 2014.

[52] Q. H. Alsafasfeh and M. S. Al-Arni, "A new chaotic behavior from Lorenz and Rossler systems and its electronic circuit implementation," *Circuits Syst.*, vol. 2, no. 2, pp. 101–105, 2011.

[53] K. Su, "Dynamic analysis of a chaotic system," *Optik*, vol. 126, no. 24, pp. 4880–4886, Dec. 2015.

[54] M. Zhang and Q. Han, "Dynamic analysis of an autonomous chaotic system with cubic nonlinearity," *Optik*, vol. 127, no. 10, pp. 4315–4319, May 2016.

[55] P. Gholamin and A. H. R. Sheikhani, "A new three-dimensional chaotic system: Dynamical properties and simulation," *Chin. J. Phys.*, vol. 55, no. 4, pp. 1300–1309, Aug. 2017.

[56] Q. Lai, J. Huang, and G. Xu, "Coexistence of multiple attractors in a new chaotic system," *Acta Phys. Pol. B*, vol. 47, no. 10, pp. 2315–2323, 2016.

[57] M. Tuna and C. B. Fidan, "Electronic circuit design, implementation and FPGA-based realization of a new 3D chaotic system with single equilibrium point," *Optik*, vol. 127, no. 24, pp. 11786–11799, Dec. 2016.

[58] S. Vaidyanathan and K. Rajagopal, "Analysis, control, synchronization and LabVIEW implementation of a seven-term novel chaotic system," Tech. Rep., 2016.

[59] A. Akgul, V.-T. Pham, I. Stouboulos, and I. Kyprianidis, "A simple chaotic circuit with a hyperbolic sine function and its use in a sound encryption scheme," *Nonlinear Dyn.*, vol. 89, no. 2, pp. 1047–1061, 2017.

[60] J. P. Singh and B. K. Roy, "A more chaotic and easily hardware implementable new 3-D chaotic system in comparison with 50 reported systems," *Nonlinear Dyn.*, vol. 93, no. 3, pp. 1121–1148, Aug. 2018.

[61] A. Sambas, S. Vaidyanathan, S. Zhang, W. T. Putra, M. Mamat, and M. A. Mohamed, "Multistability in a novel chaotic system with perpendicular lines of equilibrium: Analysis, adaptive synchronization and circuit design," *Eng. Lett.*, vol. 27, no. 4, pp. 744–751, 2019.

[62] Q. Yang and X. Qiao, "Constructing a new 3D chaotic system with any number of equilibria," *Int. J. Bifurcation Chaos*, vol. 29, no. 5, May 2019, Art. no. 1950060.

[63] A. Lassoued, O. Boubaker, R. Dhifaoui, and S. Jafari, "Experimental observations and circuit realization of a jerk chaotic system with piecewise nonlinear function," in *Recent Advances in Chaotic Systems and Synchronization*. New York, NY, USA: Academic, 2019, pp. 3–21.

[64] S. Vaidyanathan, O. A. Abba, G. Betchewe, and M. Alidou, "A new three-dimensional chaotic system: Its adaptive control and circuit design," *Int. J. Automat. Control*, vol. 13, no. 1, pp. 101–121, 2019.

[65] C. H. Lien, S. Vaidyanathan, A. Sambas, S. Sampath, and M. Mamat, "A new 3-D chaotic system with four quadratic nonlinear terms, its global chaos control via passive control method and circuit design," *IOP Conf. Ser., Mater. Sci. Eng.*, vol. 621, no. 1, Oct. 2019, Art. no. 012013.

[66] T. Kapitaniak, S. Mohammadi, S. Mekhilef, F. Alsaadi, T. Hayat, and V.-T. Pham, "A new chaotic system with stable equilibrium: Entropy analysis, parameter estimation, and circuit design," *Entropy*, vol. 20, no. 9, p. 670, Sep. 2018.

[67] G. Xu, Y. Shekofteh, A. Akgül, C. Li, and S. Panahi, "A new chaotic system with a self-excited attractor: Entropy measurement, signal encryption, and parameter estimation," *Entropy*, vol. 20, no. 2, p. 86, Jan. 2018.

[68] B. A. Idowu, S. Vaidyanathan, A. Sambas, and S. O. Onma, "A new chaotic finance system: Its analysis, control, synchronization and circuit design," in *Nonlinear Dynamical Systems with Self-Excited and Hidden Attractors*. Cham, Switzerland: Springer, 2018, pp. 271–295.

[69] H. Jinjie and S. Guangming, "A new chaotic system and its synchronization with phase spatial rotation," in *Proc. Chin. Control Decis. Conf. (CCDC)*, Jun. 2018, pp. 193–196.

[70] Q. Lai, A. Akgul, M. Varan, J. Kengne, and A. T. Erguzel, "Dynamic analysis and synchronization control of an unusual chaotic system with exponential term and coexisting attractors," *Chin. J. Phys.*, vol. 56, no. 6, pp. 2837–2851, Dec. 2018.

[71] P. C. Parks, "A new proof of the routh-hurwitz stability criterion using the second method of Liapunov," *Math. Proc. Cambridge Phil. Soc.*, vol. 58, no. 4, pp. 694–702, Oct. 1962.

KHALED BENKOUIDER received the M.S. degree in automatic control and the Ph.D. degree from the University of Jijel, Jijel, Algeria, in 2015 and 2021, respectively. His M.S. research was on secure communications-based on chaotic systems. His research interests include dynamical systems, control systems, delayed systems, LPV systems, chaotic systems synchronization, transmission security, and watermarking.

TOUFIK BOUDEN received the Engineer Diploma, M.Sc., and Ph.D. degrees in automatics and signal processing from the Electronics Institute of Annaba University, Algeria, in 1992, 1995, and 2007, respectively. He was the Head of the Non Destructive Testing Laboratory, Jijel University, Algeria. He is currently a Full Professor with the Automatics Department. His research interests include signal and image processing adapted to non-destructive testing and materials characterization, biometry, transmission security and watermarking, transmission, fractional system analysis, synthesizes, and control.

ACENG SAMBAS received the Ph.D. degree in mathematics from Universiti Sultan Zainal Abidin (UniSZA), Malaysia, in 2020. He has been a Lecturer with the Muhammadiyah University of Tasikmalaya, Indonesia, since 2015. His current research interests include dynamical systems, chaotic signals, electrical engineering, computational science, signal processing, robotics, embedded systems, and artificial intelligence.

MOHAMAD AFENDEE MOHAMED (Associate Member, IEEE) received the Ph.D. degree in mathematical cryptography, in 2011. He is currently working as an Associate Professor with Universiti Sultan Zainal Abidin. His research interests include both theoretical and application issues in the domain of data security, and mobile and wireless networking.

IBRAHIM MOHAMMED SULAIMAN received the Ph.D. degree from Universiti Sultan Zainal Abidin, Malaysia, in 2018. He is currently an International Senior Lecturer with the Department of Mathematics, School of Quantitative Sciences, Universiti Utara Malaysia. Before this, he was a Postdoctoral Researcher with the Faculty of Informatics and Computing, Universiti Sultan Zainal Abidin. He has published research articles in various international journals and attended international conferences. His research interests include optimization methods, fuzzy nonlinear systems, and numerical methods.

MUSTAFA MAMAT received the Ph.D. degree from Universiti Malaysia Terengganu (UMT), in 2007, with specialization in optimization. He has been a Professor and the Dean of the Graduate School, Universiti Sultan Zainal Abidin (UniSZA), Malaysia, since 2013. He was first appointed as a Lecturer with UMT, in 1999. Later on, he was appointed as a Senior Lecturer, in 2008, and then as an Associate Professor, in 2010, also at UMT. To date, he has successfully supervised more than 60 postgraduate students and published more than 150 research papers in various international journals and conferences. His research interests include conjugate gradient methods, steepest descent methods, Broydens family, and quasi-Newton methods.

MOHD ASRUL HERY IBRAHIM was born in Kelantan, Malaysia. He received the B.Sc. degree in financial mathematics and the M.Sc. degree in applied mathematics from Universiti Malaysia Terengganu, Malaysia. He is currently pursuing the Ph.D. degree in mathematical sciences with Universiti Sultan Zainal Abidin. He is also working with Universiti Malaysia Kelantan as a Senior Lecturer and the Director of the Publication and Rating Division. He writes regularly and has published more than 50 scientific articles in journals, and national and international conferences. His current research interests include optimization, numerical analysis, business mathematics, and business statistics.

• • •